Multi-Mode Control for Photovoltaic Grid-connected Interleaved Flyback Micro-inverters to Achieve High Efficiency in Wide Load Range*

Zhiliang Zhang, *Member*, *IEEE*, Xiao-Fei He, Xiaoyong Ren, *Member IEEE* and Xin Li
Jiangsu Key Laboratory of New Energy Generation and Power Conversion
Nanjing University of Aeronautics and Astronautics
Nanjing, Jiangsu, P. R. China
zlzhang@nuaa.edu.cn and giftxiaofei@nuaa.edu.cn

Yan-Fei Liu, *Senior Member, IEEE*

Department of Electrical and Computer Engineering
Queen's University
Kingston, Ontario, Canada
yanfei.liu@queensu.ca

***Abstract*—Boundary Conduction Mode (BCM) and Discontinuous Conduction Mode (DCM) control strategies are widely used for the flyback micro-inverter. BCM and DCM control strategies are investigated for the interleaved flyback micro-inverter concentrating on the loss analysis under different load condition. These two control strategies have different impact on the loss distribution and thus the efficiency of the flyback micro-inverter. Based on the loss analysis, a new hybrid control strategy combing the two-phase DCM and one-phase DCM control is proposed to improve the efficiency in wide load range by reducing the dominant losses depending on the load current. The experimental results verified the benefits of the proposed control.**

Keywords-micro-inverter; grid-connected; interleaved flyback;

I. INTRODUCTION

The interest in exploring renewable energies has grown in the last years due to the energy crisis. Photovoltaic (PV) sources are predicted to have the highest increase 30% in the next decade and to be the biggest contributor on the electricity generation in 2040 [1]. PV AC module, which is also called micro-inverter, is becoming more and more popular. Compared to conversational centralized, string and multi-sting inverters, micro-inverters has several advantages like higher maximum power point tracking (MPPT) efficiency and lower manufacturing cost through mass production, as well as safe and simple installation [2].

With the rapid development of the market, more and more researchers have focus on the topologies and control methods of the micro-inverters. The topologies of the single-phase grid-connected PV inverters are reviewed in [3]–[4]. The micro-inverter derived from the flyback converter, named as the flyback inverter, is widely used to its simple structure, lower cost and higher efficiency [5]. A single stage flyback inverter with the center-tapped secondary winding was presented in [6]. Each of the secondary winding transfers the energy to the AC side during a half line period with two additional MOSFETs. A modulated flyback DC/DC converter followed by a CSI was presented in [7]-[8]. The SCRs are used in the unfolding stage to reduce the cost and conduction loss. To further improve the efficiency, soft-switching， active clamp and synchronous rectifier technology were adopted in [9]-[11].

A dual mode switching strategy for the center-tapped secondary winding flyback inverter was presented in [12]-[13]. BCM and DCM modulation methods were used simultaneously during a half line period, because BCM is suitable to high power levels and DCM is better for low power levels as far as the efficiency is concerned. Owing to the combined control strategy, better efficiency could be achieved over the conventional BCM control method without additional cost. However, the power range of the BCM and DCM are applied to is not clarified regarding to the interleaved micro-inverters. More importantly, the boundary condition of the hybrid control with BCM and DCM is not analyzed, which is so important to design the power stage and the controller for the optimization of the overall performance.

In this paper, the BCM and DCM control strategies are investigated of the interleaved flyback micro-inverter concentrating on the loss analysis under different load condition respectively. It is noticed that the DCM control strategy achieves higher efficiency over BCM for the interleaved flyback micro-inverter within the power range of 200 W. The advantages of two-phase DCM operation are the current sharing and the reduction of the current stress between two interleaved phases so that the conduction loss of the power MOSFETs and diodes as well as the copper loss of the transformer can be reduced when the load current is high. On the other hand, the advantage of one-phase DCM operation is the reduction of the transformer core loss, the driving loss and turn-off loss of the power MOSFETs. To a certain power level, the output power is a pulsating power following a squared sine wave. Therefore, two-phase DCM and one-phase DCM can be used simultaneously according to different output power during a half line period. Basically, when the output power is less than a certain value, one phase needs to be shut down to reduce the dominant losses. Combing the two-phase DCM and one-phase DCM control, a new hybrid control method is proposed for the interleaved flyback micro-inverter to achieve high efficiency in wide load range. Moreover, the proposed

*This work is supported by the Public Research Funding from Jiangsu Key Laboratory of New Energy Generation and Power Conversion and the Technology Foundation for Selected Overseas Chinese Scholar from Ministry of the Industry and Information Technology.

control method is compatible with the digital implementation and requires no additional auxiliary circuitry.

II. ANALYSIS OF FLYBACK INVERTER UNDER BCM AND DCM

A. Topology of the Interleaved Flyback Micro-Inverter

Fig.1 shows the main circuit of the interleaved flyback inverter. The inverter comprises of two-phase interleaved flyback converters and a CSI. S_1 and S_2 are the power switches; D_1 and D_2 are the rectifier diodes; N_{P1} and N_{P2} are the primary windings, and N_{S1} and N_{S2} are the secondary windings. S_3-S_6 form the CSI to unfold the rectified sinusoidal waveform into the grid. S_3 and S_6 turn on during the positive half grid period while S_4 and S_5 turn on during the negative half grid period.

Fig.2 shows the current waveforms of the interleaved flyback inverter. Each phase is 180° phase-shifted in one switching period to achieve ripple cancellation. Thus a lower output filter inductance can be used.

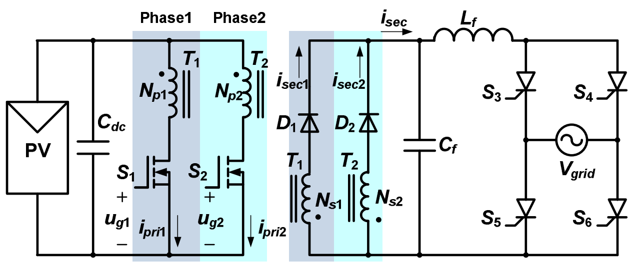

Fig.1 Main circuit of the interleaved flyback inverter

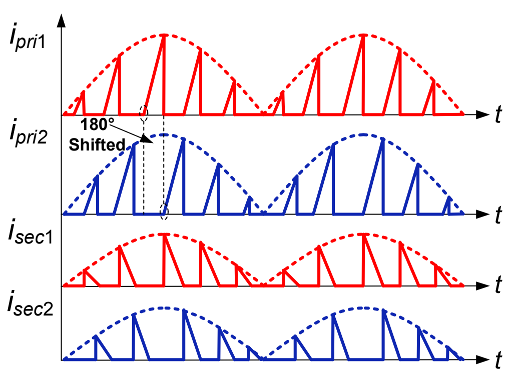

Fig.2 Key waveforms of the interleaved flyback inverter

B. Comparision of BCM and DCM

Although the SiC diodes can be used to eliminate the secondary diode reverse recovery when the flyback inverter is under CCM, they increase the cost significantly as a PV AC module. As a result, BCM and DCM control strategies are widely used for interleaved flyback micro-inverter.

The dominant losses with heavy load include the conduction loss of the MOSFETs and diodes, and the core loss and copper loss of the transformer, while the dominant losses with light load include the driving loss, turn-off loss of the MOSFETs and the transformer core loss. The range of the switching frequency increases dramatically as the power level decreases for the flyback micro-inverter under BCM. This causes the driving loss and turn-off of the MOSFETs to increase significantly. Therefore, the efficiency under BCM is much lower than DCM under light load condition. Fig.3 shows the loss distribution comparison under BCM and DCM under half load condition. It is noted that the turn off loss (P_{off}) and the gate driving loss (P_{drive}) under BCM are much higher than DCM. This translates into a significant reduction of the light load efficiency. As an example, Fig.4 shows the calculated efficiency of the interleaved flyback micro-inverter under DCM and BCM respectively.

Based on the above analysis, it should be pointed that for the interleaved flyback micro-inverter, within the power range of 200 W, DCM has the advantage over BCM. However, under heavy load condition, BCM control exhibits higher efficiency over the DCM control. Actually, the exact boundary condition between BCM and DCM operation depends on the specific application and design requirements. It should be noted that even under DCM, the micro-inverter suffers a low efficiency when the load current reduces. It should be also pointed that for the interleaved flyback micro-inverter under BCM, both primary and secondary current of the transformer need to be sensed.

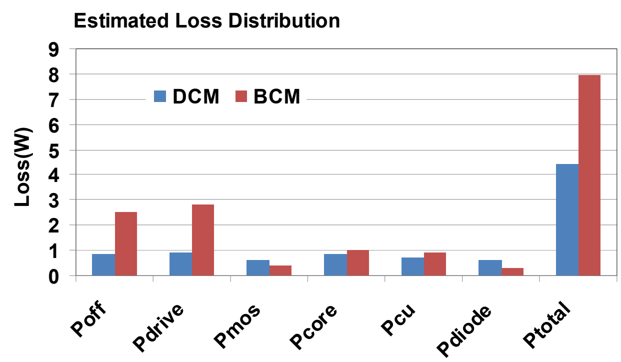

Fig.3 Loss distribution under BCM and DCM: half load condition

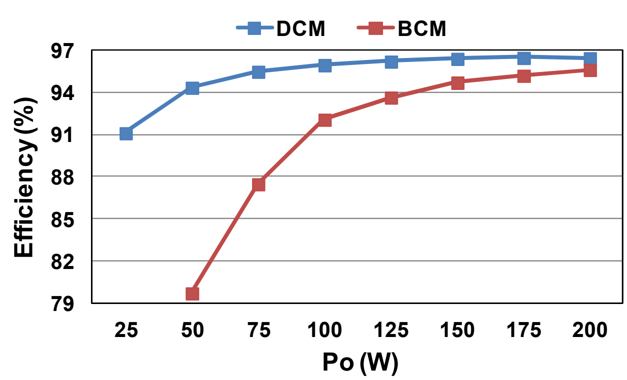

Fig.4 Calculated efficiency comparison under DCM and BCM

III. PROPOSED CONTROL METHOD AND PRICIPLE OF OPERATION

A. *Loss Analysis of DCM*

Fig.5 shows the calculated loss distribution of a 200 W interleaved flyback inverter under 100% and 25% load respectively. From Fig.5, it is observed that the dominant losses with heavy load include the conduction loss of the power MOSFETs P_{mos} and diodes P_{diode}, the transformer core loss P_{core} and copper loss P_{cu}, whereas the dominant losses with light load include the gate driving loss P_{drive}, the turn-off loss P_{off} of the power MOSFETs and the transformer core loss P_{core}. Therefore, minimizing the dominant losses according to load condition is an effective way to optimize the efficiency in wide load range.

For simplicity, 1Φ DCM represents only one phase operation and 2Φ DCM represents two phases operation under the interleaved mode. On the one hand, the 2Φ DCM operation shares the current and reduces the current stress between two interleaved phases. This is beneficial to reduce the conduction loss of the power MOSFETs and diodes, as well as the copper loss of the transformer under heavy load condition. On the other hand, the 1Φ DCM operation shields the additional phase of the micro-inverter, which minimizes the gate driving loss and the turn-off loss of the power MOSFETs as well as the core loss of the transformer under light load condition.

Based on the loss analysis, Fig.6 shows the efficiency of the interleaved flyback inverter under 1Φ DCM and 2Φ DCM operation. It is noted that the efficiency improves while operating under 1Φ DCM within the power range of 100 W. Actually, 2Φ DCM and 1Φ DCM can be used simultaneously to modulate the interleaved flyback inverter depending on the load current during a half line period.

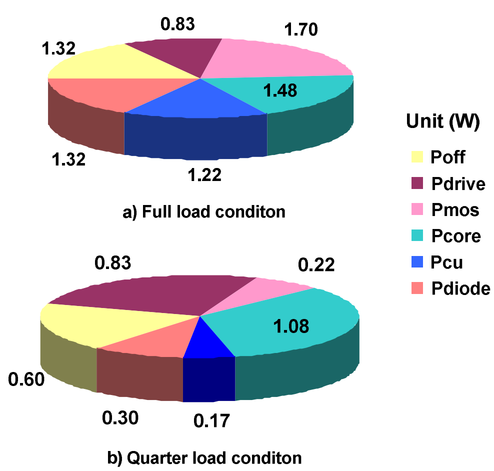

Fig.5 Calculated power losses of interleaved flyback inverter

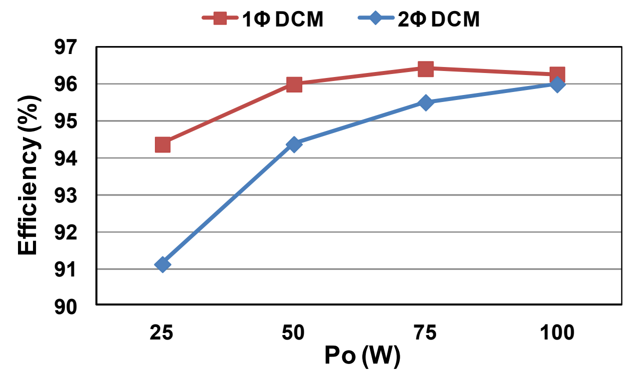

Fig.6 Calculated efficiency of interleaved flyback inverter

B. *Proposed Hybrid Control Method*

From the analysis above, it is interesting to notice that the advantage of 2Φ DCM operation is current sharing between two phases and the conduction loss of the power MOSFETs and diodes and the copper loss of the transformer can be reduced when the load current is high. The 1Φ DCM operation reduces the driving loss and turn-off loss of the power MOSFETs and the transformer core loss. The conventional DCM control only shields one phase when the load reduces to some power level. Actually, during the half line period, either 2Φ DCM or 1Φ DCM control can be applied. It is noticed that the output power P_{out} during a half line period is a pulsating power following a squared sine wave. The output power P_{out} in a half line frequency period is

$$P_{out} = 2P_o \sin^2(\omega t) \quad (1)$$

where P_o presents the average of the output power.

The idea here is to combine the advantages of 2Φ DCM and 1Φ DCM adaptively to the load current during a half line period with the phase shielding technology, so that the efficiency can be optimized in wide load rang.

Fig.7 shows the operating region of 1Φ DCM and 2Φ DCM during a half line period.

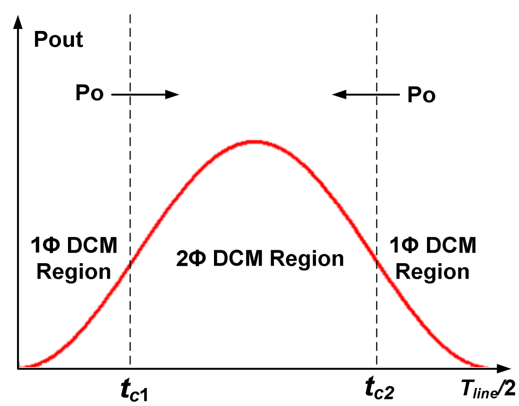

Fig.7 The output power curve with 1Φ and 2ΦDCM for the interleaved flyback micro-inverter

In Fig.7, 2Φ DCM is employed when load current is high and 1Φ DCM is employed when the load current under a certain level. In this way, the dominant losses are reduced depending on the load current and higher efficiency can be achieved in wide load range. Moreover, the proposed control is compatible with the digital implementation without additional cost. It should be noted that as P_o decreases, the 2Φ DCM region decreases simultaneously. In particular, when P_o decreases to a certain level, the hybrid modulation merges into only 1Φ DCM.

C. Design and Analysis of Reference Signal

For the proposed control method, the reference signal i_{ref} should be well designed to achieve a higher efficiency and a lower THD performance. Since the equivalent circuit of the two modules is similar, DCM of a single phase flyback will be analyzed firstly. Fig.8 shows the equivalent circuit of single flyback inverter during a half line period.

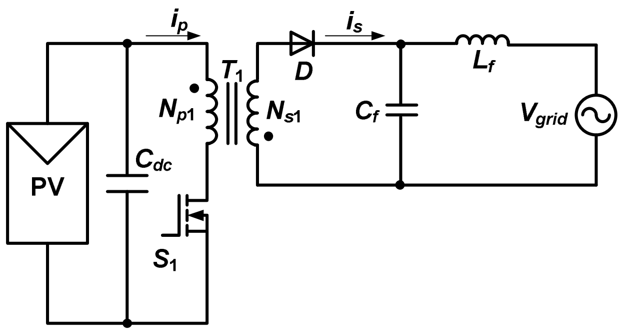

Fig.8 Equivalent circuit of one single flyback

During the S_1 on time, the primary current i_p increases gradually in a linear relationship with V_{dc} and L_p. During the S_1 off time, second current i_s decreases in a linear relationship with V_g (t) and L_s. According to these, the turn-on time Ton and the turn-off time Toff are

$$T_{on} = \frac{L_p \cdot I_p}{V_{dc}} \tag{2}$$

$$T_{off} = \frac{L_s \cdot I_s}{V_g(t)} \tag{3}$$

I_p and I_s represent the peak value of i_p and i_s respectively. I_p equals to the reference signal i_{ref}. So two relationships of I_p and I_s are

$$I_p = i_{ref} \tag{4}$$

$$I_s = I_p \cdot \sqrt{\frac{L_p}{L_s}} = i_{ref} \cdot \sqrt{\frac{L_p}{L_s}} \tag{5}$$

The output current i_{out} equals to secondary current i_s. There is an approximation relation, which is the RMS value of i_{out} equals approximately to the average value in every switching cycle.

$$i_{out} = \frac{I_s \cdot T_{off}}{2T_s} \tag{6}$$

Considering all the equations above, the relationship between i_{out} and i_{ref} is

$$i_{ref} = \sin(\omega t)\sqrt{\frac{2I_{out} \cdot V_p}{L_p \cdot f_s}} = 2\sin(\omega t)\sqrt{\frac{P_o}{L_p \cdot f_s}} \tag{7}$$

For the interleaved flyback inverter with the proposed control method, the current reference i_{ref1} and i_{ref2} during a half line period are

$$i_{ref1} = \begin{cases} 2\sqrt{2}\sin(\omega t)\sqrt{\dfrac{P_o}{L_p \cdot f_s}} & (t < t_{c1}, t > t_{c2}) \\ 2\sin(\omega t)\sqrt{\dfrac{P_o}{L_p \cdot f_s}} & (t_{c1} < t < t_{c2}) \end{cases} \tag{8}$$

$$i_{ref2} = 2\sin(\omega t)\sqrt{\frac{P_o}{L_p \cdot f_s}} \quad (t_{c1} < t < t_{c2}) \tag{9}$$

While t_{c1} and t_{c2} can be calculated from (10) as shown in Fig.7.

$$\sin(\omega t_{c1}) = \sin(\omega t_{c2}) = \sqrt{\frac{100}{4P_o}} \tag{10}$$

D. Control Diagram of Interleaved Flyback Micro-Inverter

Fig.9 shows the control block diagram of interleaved flyback inverter based on the analysis above. The control blocks are implemented by Freescale DSP MC56F8257. In the diagram, Phase Locked Loop (PLL) is used to detect the phase angle, amplitude and frequency of the grid voltage, while islanding protection is used to guarantees the inverter under normal utility condition. MPPT block is used to calculate the input power and the result is P_o, which is use to adjust the i_{ref}.

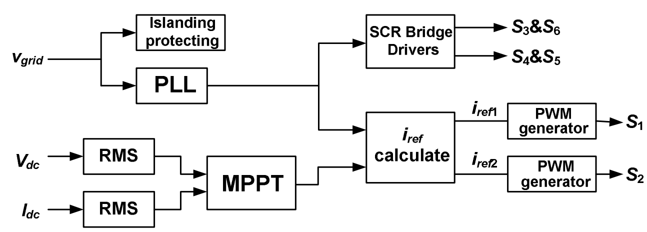

Fig.9 Control diagram of interleaved flyback micro-inverter

IV. Experimental Results and Discussion

To verify the proposed hybrid control method, a prototype of 200 W has been built. A PV array simulator is used as an input source. The parameters of the interleaved flyback micro-inverter are listed in Table I.

Table I Circuit parameters of interleaved flyback micro-inverter

Input voltage V_{dc}	36~60 V	Filter inductance L_f	600 μH
Output power P_o	200 W	Filter capacitance C_f	0.33 μF
Primary inductance L_p	28 μH	Grid voltage V_{grid}	220 V
Turn ratio N (N_s/N_p)	2	Switching frequency f_s	100 kHz

Fig.10 shows the key waveforms of the interleaved flyback micro-inverter with the proposed hybrid control method under full load condition. During a line period, when the output power P_{out} under a certain value (100 W), one phase is shut down in order to minimize the overall loss. The envelop of the primary current i_{p1} and i_{p2} equal to the designed reference signal i_{ref1} and i_{ref2} as shown in Fig.10 (a). Fig.10 (b) shows that the micro-inverter works under an interleaved operation mode at 2Φ DCM region.

Fig.11 and Fig.12 show the key waveforms similar to Fig.10 under half load and quarter load condition respectively. Comparing Fig.11 (a) to Fig.10 (a), it is observed that as the power level decreases, the 2Φ DCM region decreases accordingly. When the power level decreases below 50 W, the hybrid modulation with 2Φ DCM and 1Φ DCM merges into only 1Φ DCM region as shown in Fig.12 (a). This means the proposed control has the capability to achieve phase-shielding inherently.

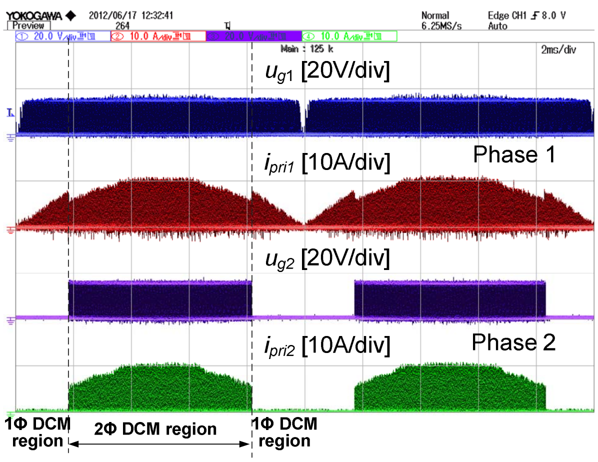

(a) Gate drive voltage and primary current of Phase 1 and Phase 2

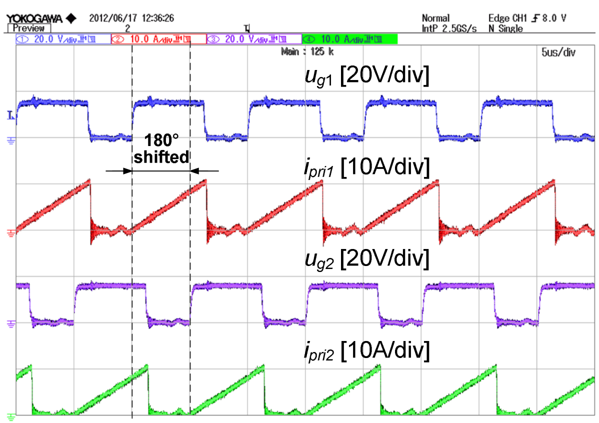

(b) Gate drive voltage and primary current of Phase 1 and Phase 2 (expanded)

Fig.10 Key Waveforms: Full Load Condition

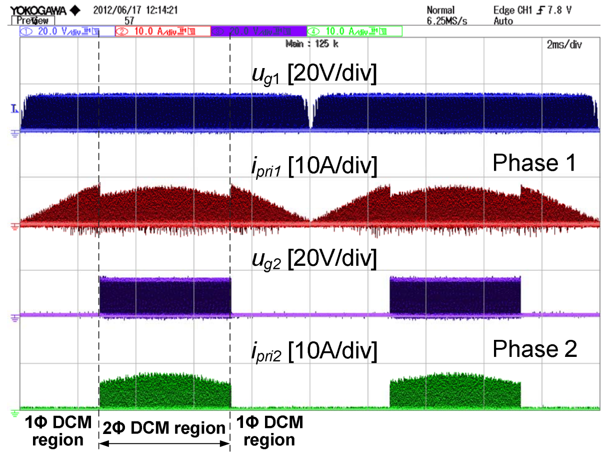

(a) Gate drive voltage and primary current of Phase 1 and Phase 2

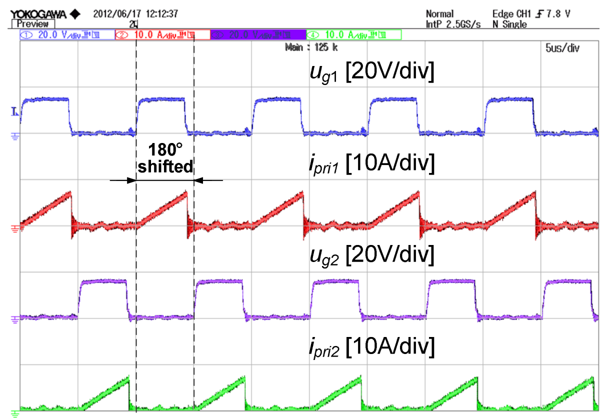

(b) Gate drive voltage and primary current of Phase 1 and Phase 2 (expanded)

Fig.11 Key Waveforms: Half Load Condition

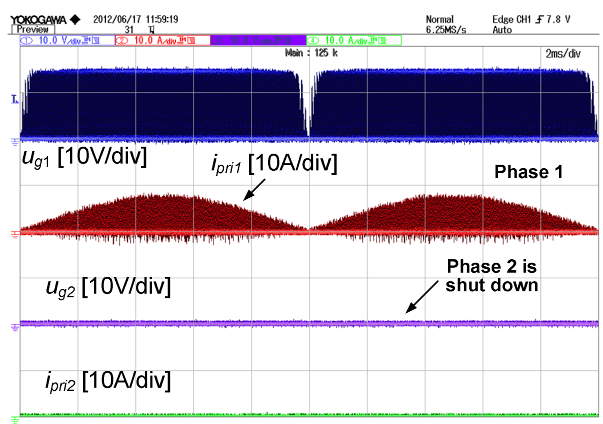

(a) Gate drive voltage and primary current of Phase 1 and Phase 2

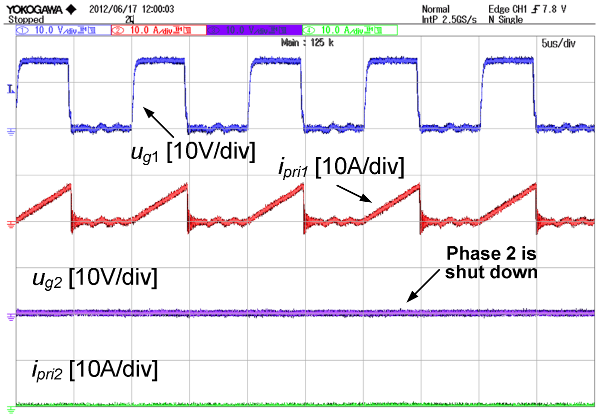

(b) Gate drive voltage and primary current of Phase 1 and Phase 2 (expanded)

Fig.12 Key Waveforms :Quarter Load Condition

Fig.13 shows the efficiency of the conventional control method and the proposed hybrid control method. With light load as P_o is 50 W, the hybrid modulation with 2Φ DCM and 1Φ DCM merges into only 1Φ DCM region. The driving loss and turn-off loss of the power MOSFETs and the transformer core loss are reduced and the efficiency can be improved by 4% over the conventional two-phase interleaved operation mode. With heavy load as P_o is 200 W, the 1Φ DCM region reduces and the overall loss doesn't reduce that much. But the efficiency is still improved by 0.5%.

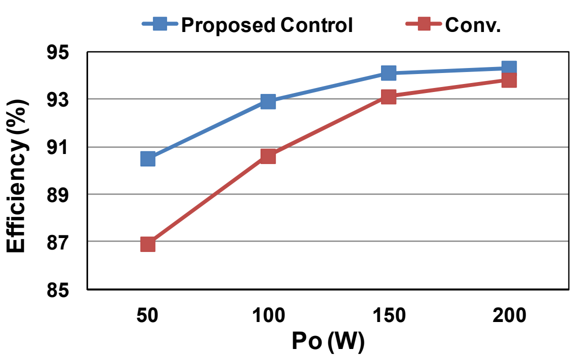

Fig.13 Efficiency of conventional control and proposed hybrid control

V. Conclusion

In this paper, the loss distribution and the efficiency of the interleaved flyback micro-inverter under BCM and DCM are investigated analytically under different power levels. It is found that DCM is a better choice than BCM within the power range of 200 W. For the interleaved flyback micro-inverter, the dominant losses with heavy load include the conduction loss of the power MOSFETs and diodes, and the core loss and copper loss of the transformer; while the dominant losses with light load include the gate driving loss, turn-off loss of the power MOSFETs and the transformer core loss. The 2Φ DCM operation shares the current and reduces the current stress between two interleaved phases. The conduction loss of the power MOSFETs and diodes and the copper loss of the transformer can be reduced at heavy load, and the 1Φ DCM reduces the driving loss and the turn-off loss of the main MOSFETs and the core loss of the transformer under light load condition. A new hybrid control strategy combining the 2Φ DCM and 1Φ DCM control during a half line period is proposed. With the proposed control strategy, high efficiency can be achieved in wide load rang by reducing the dominant losses depending on the load current.

The experimental results verified the proposed control. With the proposed control, the efficiency could be improved around 4% under light load condition. Even under heavy load condition, the efficiency could be improved by 0.5%. Moreover, the proposed control method is compatible with the digital implementation and requires no additional auxiliary circuitry.

References

[1] http://www.erec.org/media/publications/2040-scenario.html

[2] P. D. Maycock, "Cost reduction in PV manufacturing: impact on grid-connected and building integrated market," Solar Energy Mater. Solar Cells, Vol. 47, No. 1-4, pp. 37-45, Oct. 1997.

[3] S. B. Kjaer, J. K. Pedersen and F. Blaabjerg, "A review of single-phase grid-connected inverters for photovoltaic modules," *IEEE Trans. on Industry Applications*, Vol. 41, No. 5, pp. 1292-1306, Sep/Oct. 2005.

[4] Q. Li and P. Wolfs, "A Review of the single phase photovoltaic module integrated converter topologies with three different DC link configurations," *IEEE Trans. on Power Electronics*, Vol. 23, No. 3, pp. 1320-1333, May 2008.

[5] N. Kutkut and H. Hu, "Photovoltaic micro-inverters: topologies, control aspects, reliability issues, and applicable standards," in *Proc. IEEE Energy Conversion Congress and Exposition (ECCE)*, 2010, tutorial.

[6] A. C. Kyritsis, E .C. Tatakis and N. P. Papanikolaou, "Optimum design of the current-source flyback inverter for decentralized grid-connected photovoltaic systems," *IEEE Trans. on Energy Conversion*, Vol. 23, No. 1, pp. 281-293, March 2008.

[7] J. Y. Gu, H. F. Wu, G. C. Chen and Y. Xing, "Research on photovoltaic grid-connected inverter based on soft-switching interleaved flyback converter," in *Proc. IEEE Conference on Industrial Electronics and Applications*, 2010, pp. 1209-1214.

[8] M. Gao, M. Chen, Q. Mo, Z. Qian and Y. Luo, "Research on output current of interleaved-flyback in boundary conduction mode for photovoltaic AC module application," in *Proc. IEEE Energy Conversion Congress and Exposition (ECCE)*, 2011, pp. 770-775.

[9] Q. Mo, M. Chen, Z. Zhang, Y. Zhang and Z. Qian, "Digitally controlled active clamp interleaved flyback converters for improving efficiency in photovoltaic grid-connected micro-inverter," in *Proc. IEEE Applied Power Electronics Conference and Exposition (APEC)*, 2012, pp. 555-562.

[10] Y. H. Kim, J. G. Kim, C. Y. Won, Y. C. Jung and T. W. Lee, "Soft switching interleaved active clamp flyback inverter for a photovaltaic AC module system," in *Proc. Eur. Conf. Power Electronics and Applications*, 2011, pp. 1-9.

[11] D. K. Ryu, Y. H. Kim, J. G. Kim, C. Y. Won and Y. C. Jung, "Interleaved active clamp flyback inverter using a synchronous rectifier for a photovoltaic AC module system," in *Proc. IEEE Interntional Conf. Power Electronics and ECCE Asia (ICPE & ECCE)*, 2011, pp. 2631-2636.

[12] Z. Zhang, M. Chen, M. Gao, Q. Mo and Z. Qian, "An optimal control method for grid-connected photovoltaic micro-inverter to improve the efficiency at light-load condition," in *Proc. IEEE Energy Conversion Congress and Exposition (ECCE)*, 2011, pp. 219-224.

[13] Y. H. Ji, D. Y. Jung, J. H. Kim, C. Y. Won and D. S. Oh, "Dual mode switching strategy of flybcak inverter for photovoltaic AC modules," in *Proc. IEEE Internationl Power Electronics Conference(IPEC)*, 2010, pp. 2924-2929.